Neurobiology of Disease xxx (2008) xxx–xxx

Contents lists available at ScienceDirect

Neurobiology of Disease

journal homepage: www.elsevier.com/locate/ynbdi

Mislocalization of h channel subunits underlies h channelopathy in temporal lobe epilepsy

Minyoung Shin [a], Darrin Brager [b], Thomas C. Jaramillo [a], Daniel Johnston [b], Dane M. Chetkovich [a,c,*]

[a] Davee Department of Neurology and Clinical Neurosciences, Feinberg School of Medicine, Northwest University Medical School, Chicago, IL 60611, USA
[b] Center for Learning and Memory, Section of Neurobiology, University of Texas at Austin, Austin, Texas 78712, USA
[c] Department of Physiology, Feinberg School of Medicine, Northwestern University Medical School, Chicago, IL 60611, USA

ARTICLE INFO

Article history:
Received 1 May 2008
Revised 11 June 2008
Accepted 13 June 2008
Available online xxxx

Keywords:
Epilepsy
Seizure
Hyperpolarization-activated cyclic
Nucleotide-gated channel
Kainic acid

ABSTRACT

Many animal models of temporal lobe epilepsy (TLE) begin with status epilepticus (SE) followed by a latency period. Increased hippocampal pyramidal neuron excitability may contribute to seizures in TLE. I_h, mediated by h channels, regulates intrinsic membrane excitability by modulating synaptic integration and dampening dendritic calcium signaling. In a rat model of TLE, we found bidirectional changes in h channel function in CA1 pyramidal neurons. 1–2 d after SE, before onset of spontaneous seizures, physiological parameters dependent upon h channels were augmented and h channel subunit surface expression was increased. 28–30 d following SE, after onset of spontaneous seizures, h channel function in dendrites was reduced, coupled with diminished h channel subunit surface expression and relocalization of subunits from distal dendrites to soma. These results implicate h channel localization as a molecular mechanism influencing CA1 excitability in TLE.

Introduction

Temporal lobe epilepsy (TLE) is a common cause of intractable seizures (Engel, 1993), but mechanisms governing seizure propensity in TLE remain elusive. In many animal TLE models, an initial episode of status epilepticus (SE) is followed by a seizure-free interval (latent period) before spontaneous seizures commence. In TLE, seizures often originate in the hippocampus (Dudek et al., 2002; White, 2002). Thus, understanding molecular mechanisms controlling hippocampal excitability is central to developing effective therapies.

The subcellular localization of voltage-gated ion channels is critical for regulating neuronal excitability (Lai and Jan, 2006). Apical dendrites of CA1 pyramidal neurons possess a markedly polarized distribution of hyperpolarization-activated current, I_h, which is mediated by hyperpolarization-activated cyclic nucleotide-gated (HCN) channels (h channels) comprised of HCN1 and HCN2 subunits. Both I_h (Magee, 1998, 1999) and HCN1 and 2 subunits (Lorincz et al., 2002; Notomi and Shigemoto, 2004; Santoro et al., 2000) are strikingly enriched in distal dendrites. A fraction of h channels is active near the resting membrane potential, thereby depolarizing neurons. In the soma of CA1 pyramidal neurons, increased I_h can result in repetitive firing by rebound depolarization (Chen et al., 2001). In distal dendrites of CA1 pyramidal neurons, I_h limits excitability by 1) depolarization-mediated inactivation of voltage-gated Ca^{++} channels (Tsay et al., 2007), and 2) reduction of kinetic and amplitude components of EPSPs (Magee, 1998). Blocking I_h increases dendritic excitability in CA1 pyramidal neurons (Magee, 1999), whereas pharmacological enhancement of dendritic I_h reduces CA1 excitability (Poolos et al., 2002).

In CA1 pyramidal neurons, neuronal activity mediates bidirectional homeostatic control of I_h (Brager and Johnston, 2007; Fan et al., 2005; Narayanan and Johnston, 2007; van Welie et al., 2004). Along these lines, we and others have observed that activity controls h channel localization in CA1 pyramidal neurons (Bender et al., 2007; Shin and Chetkovich, 2007). Recently, Jung et al. reported a chronic increase in CA1 pyramidal neuron excitability due to reduced I_h in CA1 dendrites in the pilocarpine model of TLE, and suggested that diminished h channel expression underlies this defect (Jung et al., 2007). To further address the mechanism of h channel dysfunction in TLE, we explored whether h channel trafficking is altered during TLE epileptogenesis.

Our results demonstrate an increase in I_h in CA1 pyramidal neurons 1–2 d after SE, an effect explained by an upregulation of HCN1 surface expression. At 28–30 d after SE, I_h is significantly reduced in dendrites, and h channels are downregulated from the surface membrane. Furthermore, HCN1 subunits are mislocalized from dendrites to the soma, and interaction between HCN1 and a protein implicated in h channel trafficking, TRIP8b, is disrupted. These findings suggest that aberrant h channel subunit trafficking contributes to the h channelopathy in TLE.

* Corresponding author. Davee Department of Neurology and Clinical Neuroscience, Northwestern University Medical School, 303 East Chicago Avenue, Ward 10-201, Chicago, IL 60611-3008, USA. Fax: +1 312 503 0872.
E-mail address: d-chetkovich@northwestern.edu (D.M. Chetkovich).
Available online on ScienceDirect (www.sciencedirect.com).

0969-9961/$ – see front matter © 2008 Elsevier Inc. All rights reserved.
doi:10.1016/j.nbd.2008.06.013

Materials and methods

Animals and induction of SE

8–12 week old Sprague–Dawley male rats were purchased (Charles River Laboratories, Wilmington, MA) and maintained in 12L/12D cycle. SE was induced by injection of kainic acid (10 mg/kg, Tocris, Ellisville, MO) intraperitoneally. Behavior of animals was observed, and seizures were scored according to the Racine scale from class III (wet dog shake) to class V (rearing, falling, tonic–clonic seizures) (Racine, 1972). 1 h after onset of SE, seizures were aborted by injecting sodium pentobarbital (30 mg/kg, Abbott laboratories, North Chicago, IL) subcutaneously. The Northwestern University (NUACUC) and the University of Texas at Austin Animal Care and Use Committee (IACUC) approved all animal usage in these studies.

Surgery to implant EEG leads

For surface EEG recording, rats were anesthetized with ketamine/xylazine, burr holes made and electrodes [stainless steel screw soldered to a silver connection wire (MedWire, Mt. Vernon, NY)] placed apposing the dura for 2 EEG channels: 1) over the left frontal and occipital cortex, and 2) over the left and right frontal cortex. For intrahippocampal EEG recording, rats were positioned into a stereotaxic frame (Kopf Instruments, Tujunga, CA), and a midline incision was made exposing the scalp. Two holes were drilled in the skull for bilateral hippocampal placement (5.28 mm posterior, 4.5 mm lateral to bregma and 3.2 mm below brain surface) of EEG stainless steel Teflon coast blunt cut wires. Each EEG wire was securely attached to the skull using dental cement. Additionally a hole was drilled ventral to the two EEG wires for the placement of self-tapping stainless steel anchor screw, of which an uncoated wire was wrapped around serving as the ground. For both surface and intrahippocampal recordings, two EMG wires were also placed into the neck muscle. Finally a multi channel electrode unit (Plastics One, Roanoke, VA) to which all wires were soldered was securely attached with superglue onto the top of the skull. All wires were further covered with dental cement and the lesion was sutured. Following surgery, buprenorphine hydrochloride (0.07 ml, i.m.; 0.3 mg/ml) was given for analgesia. Recordings for all rats began 14 d following the initial surgical procedure.

Video/EEG recording of seizures

After recovery from surgery, rats were connected to a wire tether and integrated preamplifier unit (Pinnacle, Lawrence, KS). All signals were amplified 100× at the preamplifier before the tether and swivel arrangement, and 100× at the main amplifier stage (10,000× total); EMG signals were amplified an additional 50× (5,000× total). EEG channels were filtered at 0.5 Hz high pass and 50 Hz low pass; EMG signals were filtered at 10/200 Hz, and a 60 Hz digital notch filter is applied to all channels. Sampling at 400 Hz is digitized using a 14-bit A/D converter (Texas Instruments), collected and stored on a desktop PC running the Sirenia software (Pinnacle).

Video and EEG/EMG recordings were obtained for 30 min on 8–12 week old Sprague–Dawley rats to obtain a baseline recording, then status epilepticus was induced by injection of kainic acid (10 mg/kg i.p.). Electrographic status epilepticus was defined as continuous high amplitude sharp-wave activity >2 fold above pre-KA baseline amplitudes. For continuous recordings, video and EEG data was evaluated off-line for the preceding 24 hr period; First spontaneous seizure was defined behaviorally as Racine class III or greater (unilateral clonic activity, bilateral tonic–clonic forelimb activity or generalized tonic–clonic activity) or electrographically as repetitive rhythmic (2–8 Hz) high amplitude (>2 fold above background) sharp-wave activity lasting longer than 10 seconds.

Antibody generation

cDNA encoding mouse TRIP8b was generously provided by Drs. Bina Santoro and Steven Siegelbaum (Columbia University, New York, NY) (Santoro et al., 2004). cDNA encoding amino acids 1–190 of mouse TRIP8b (Accession number: NM_021483) was generated by PCR using primers (5′-CGC GAA TTC ATG TCT GAC AGT GAA and 3′-GCG CTC GAG AGA TCT GTG TTC TGC GG), followed by subcloning the PCR product into the EcoRI/XhoI sites of the glutathione-*S*-transferase-producing vector, pGEX-4T1 (Pharmacia, Piscataway, NJ). The resulting GST-TRIP8b(1–190) fusion protein was expressed in BL21 bacteria (Stratagene, La Jolla, CA) and purified by Glutathione-sepharose affinity chromatography according to the manufacturer's protocol (Amersham Biosciences, Piscataway, NJ). Rabbits were immunized (Affinity Bioreagents, Golden, CO) with the GST-TRIP8b(1–190) fusion protein to generate immune and pre-immune serum, and one animal yielded the sensitive and specific serum used in these studies (rab α-TRIP8b).

Immunohistochemistry

Rats were anesthetized by inhalation of halothane and perfused with freshly depolymerized 4% paraformaldehyde in 0.1 M phosphate buffer (PFA-PBS). Brains were rapidly removed and post-fixed for 24 h, then free-floating sections (50 μm) were cut on a vibratome (Leica, Nussloch, Germany). Staining was performed with the gp α-HCN1 (Shin and Chetkovich, 2007), gp α-HCN2 (Shin et al., 2006) (each 1:1000), mouse α-Kv4.2 (1:50, NeuroMab, Davis, CA), or rab α-TRIP8b (1:10,000) followed by species-specific secondary antibody in an avidin–biotin–peroxidase system (ABC Elite; Vector laboratories). Peroxidase staining was developed using 3,9-diaminobenzidine (DAB) as the chromogen. For fluorescence immunohistochemistry, sections were incubated with gp α-HCN1 or gp α-HCN2 and mouse α-PSD95 (1:1000, NeuroMab, Davis, CA). Next, sections were incubated with α-gp-alexa488 (Molecular Probes, Carlsbad, CA) and α-mouse-cy3 (Jackson ImmunoResearch Laboratories, Inc., West Grove, PA) to visualize the primary antibodies. Sections were mounted with Vectashield (Vector laboratories, Burlingame, CA).

Light microscopy

Digital images of DAB-stained sections were taken with 3× or 8× objectives affixed to a Nikon SMZ 1000 microscope with SPOT Advance software, equipped with RT slider camera (Diagnostic Instruments, Inc., Sterling Heights, MI). All images were exported and analyzed using NIH image J software.

Fluorescence light microscopy and data analysis

Digital images were taken with a 5× objective (NA = 1.4) affixed to a Zeiss Axiovert 200M inverted microscope with Axiovision 3.0 software driven controls, equipped with an Axio Cam HRm camera. Pairs of control and SE tissue sections were stained at the same time with the same aliquots of block, primary and secondary antibodies, and pictures were taken with identical exposure time and objective under the same microscope. HCN subunit spatial distribution was quantified utilizing NIH Image J software. Area CA1 was identified (by the thin pyramidal layer and relationship to dentate gyrus (DG) blades) and bisected with a line across CA1 perpendicular to the pyramidal cell body layer. Three sections were defined: apical dendrites, soma, and basilar dendrites. The segments comprising basilar and apical dendrites were divided into 3 and 10 equal sections, respectively, and average pixel intensity in each sub-segment (as well as for the pixels across the soma) was assigned to the distal (with respect to the soma) point of each division. H channel subunit (or control protein) immunoreactivity was analyzed across CA1 along the bisection line

Please cite this article as: Shin, M., et al., Mislocalization of h channel subunits underlies h channelopathy in temporal lobe epilepsy, Neurobiol. Dis. (2008), doi:10.1016/j.nbd.2008.06.013

using the "plot profile" function. The data file was used to graph *X* as distance from soma, and *Y* as intensity of pixels. Division in equal subsegments allowed comparison between different animals that may have been sectioned in slightly different planes or angles and hence have different lengths of dendritic fields; data was represented as relative pixel intensity (normalized to the lowest average pixel value of a sub-segment or the soma for each slice, minus background signal from an area of the image lacking tissue, e.g. the hippocampal fissure). Each data point (*n*) reflected the average segmental intensity of 5 bisection lines from sections of a single experimental or control brain. ANOVA with post hoc analysis using Tukey Honest Significant Difference was used to evaluate statistical significance (Graphpad Software, San Diego, CA).

Coimmunoprecipitation assay

Acute hippocampal slices (400 μm) from control or SE animals were prepared and area CA1 was dissected for further study. Protein extracts were generated in TEEN-Tx, and antibodies (gp α-HCN1, gp α-HCN2, gp α-HCN4, rab α-TRIP8b) were added for 2 h at 4 °C, then pre-washed protein A beads (Sigma, MO) were added and samples incubated for another 2 h at 4 °C. Beads were precipitated and washed 3 times with TEEN-Tx then eluted in SDS-containing sample buffer and boiled for 2 min prior to SDS-PAGE.

Biotinylation of acute hippocampal slices

400 μm thick-acute hippocampal slices were prepared from control or SE animals. Tissues were rinsed in cold PBS and incubated with 1 mg/ml sulfo-NHS-LC-biotin (Pierce, Rockford, IL) for 30 min at 4 °C to label surface expressed proteins. Excess biotin was quenched with 20 mM NH_4Cl in PBS, and tissue extracts were generated in TEEN-Tx. Biotinylated proteins were precipitated by incubating tissue extracts with neutravidin beads (Pierce, Rockford, IL), and then eluted in DTT-containing protein sample buffer.

Western blotting

Protein extracts from dissected hippocampal area CA1 were resolved by SDS-PAGE and transferred to PVDF membranes (Millipore, Billerica, MA). Primary antibodies, gp α-HCN1 (1:1000), gp α-HCN2 (1:1000), rab α-TRIP8b (1:10,000), mouse α-Kv4.2 (1:100, NeuroMab, Davis, CA), rab α-GluR1 (1:1000, Millipore, Billerica, MA), α-α-tubulin (DM1A, 1:2000, Sigma, MO) and α-β-tubulin III (1:2000, Sigma, MO) were diluted in block solution containing 5% milk and 0.1% Tween-20 in TBS (TBST) and membranes were incubated in the primary antibody solution overnight at 4 °C or 1 h at room temperature (RT). Blots were washed 3×10 min with TBST, and species-appropriate secondary antibody conjugated to horseradish peroxidase (Sigma, MO) was added in TBST containing 5% milk at a dilution of 1:2500. Labeled bands were visualized using Supersignal chemiluminescence (Pierce, Rockford, IL). Densitometric quantitation of band intensity was performed using NIH Image J software.

Acute hippocampal slices

Hippocampal slices (350 μm) were prepared from control or post SE male Sprague–Dawley rats (Charles River Laboratories, Wilmington, MA) using standard techniques (Magee and Johnston, 1997). Briefly, animals were anesthetized with ketamine and xylazine. Upon deep anesthesia, intracardiac perfusion was initiated with ice-cold modified ACSF containing (in mM) 210 sucrose, 2.5 KCl, 1.2 NaH_2PO_4, 25 $NaHCO_3$, 0.5 $CaCl_2$, 7.0 $MgCl_2$, and 7.0 dextrose bubbled with 95% O_2/5% CO_2. The brain was removed and bisected along the midline. To promote an orientation favoring dendritic projection in a plane parallel to the surface of the slice, an additional cut was made on the dorsal surface at a 30 degree angle lateral to the midline. The brain was mounted and sliced using a microtome (Vibratome, St. Louis, MO). Slices were placed in a holding chamber filled with ACSF containing (mM): 125 NaCl, 2.5 KCl, 1.25 NaH_2PO_4, 25 $NaHCO_3$, 2 $CaCl_2$, 2 $MgCl_2$, and 25 dextrose (see below) warmed to 35 °C for 20 min and then placed at room temperature for <6 h until needed for recording.

Electrophysiology

Slices were placed individually as needed into a submerged recording chamber continuously perfused with control extracellular saline. Slices were viewed with a Zeiss Axioskop using infrared video microscopy and differential interference contrast (DIC) optics. For all recordings, the control ACSF solution contained (mM): 125 NaCl, 2.5 KCl, 1.25 NaH_2PO_4, 25 $NaHCO_3$, 2 $CaCl_2$, 1 $MgCl_2$, and 25 dextrose and was bubbled continuously with 95% O_2/5% CO_2 at 31–33 °C. Patch pipettes were pulled from borosilicate glass and had a resistance of 4–8 MΩ when filled with the internal recording solution containing (in mM): 120 potassium gluconate, 20 KCl, 10 HEPES, 4 NaCl, 0.2 EGTA, 4 MgATP, 0.3 TrisGTP and 14 phosphocreatine (pH 7.3 with KOH).

Whole cell current clamp recordings were made from the soma or in the apical dendrite (130–180 μm; mean=150 μm) using a Dagan BVC-700 in current clamp mode. Series resistance was monitored throughout the recording and experiments in which the series resistance exceeded 30 MΩ were discarded.

Data acquisition and analysis

Data were sampled at 10 kHz, filtered at 3 kHz and digitized by an ITC-18 interface connected to computer running custom software written in IGOR Pro (Wavemetrics). All data analyses were performed with custom written software in IGOR Pro (Wavemetrics).

Input resistance (R_N) was determined by the slope of the linear regression line through the linear range of the *V–I* plot (constructed by plotting the amplitude of the steady-state voltage against the corresponding current injection from a family of 500–750 ms current steps).

For measurements of temporal summation, simulated EPSPs (αEPSPs) were used to remove any contribution of presynaptic mechanisms. αEPSPs were simulated by the injection of current into the soma using the following function: $I = I_{max}(t/\alpha)\ e^{-\alpha t}$. I_{max} (184±15 pA) and α (0.31±0.01) were adjusted to produce EPSP-like waveforms with a peak amplitude of 5 mV and a time-to-peak of 10 ms. Temporal summation ratio was measured as the amplitude of the fifth alpha EPSP (αEPSP) relative to first in a train of 5 αEPSPs $[(\alpha EPSP_5 - \alpha EPSP_1)/\alpha EPSP_1]$.

Voltage sag was measured as the percent change between the maximum and steady-state voltage change during hyperpolarizing current injections $[(V_{max} - V_{ss})/V_{max}] \times 100$. The stimulus used for characterizing the impedance amplitude profile (ZAP) was a sinusoidal current of constant amplitude, with its frequency linearly spanning 0–15 Hz in 15 s. The magnitude of the ratio of the Fourier transform of the voltage response to the Fourier transform of the ZAP stimulus formed the impedance amplitude profile. The frequency at which the impedance amplitude reached its maximum was the resonance frequency.

Results

Induction of status epilepticus and behavioral monitoring

Seizures were induced in adult male rats using a single intraperitoneal dose of kainic acid (KA) and scored behaviorally using the Racine scale (Racine, 1972). Within 2 h of KA administration, class V seizures were observed in 90% of treated animals, and status epilepticus was confirmed electrographically in 5/5 animals exhibiting

Please cite this article as: Shin, M., et al., Mislocalization of h channel subunits underlies h channelopathy in temporal lobe epilepsy, Neurobiol. Dis. (2008), doi:10.1016/j.nbd.2008.06.013

class V seizures utilizing electroencephalography (EEG) (Supplementary Fig. 1). To limit cytotoxic injury caused by prolonged status epilepticus (Du et al., 1995; Wu and Leung, 2003) and reduce mortality, 1 h after onset of class V status epilepticus (SE), seizures were terminated by treating animals with the anticonvulsant sodium pentobarbital (PB). Consistent with prior studies utilizing KA to induce hippocampal epilepsy (Mascott et al., 1994), behavioral or electrographic seizures were not observed before 1 week following SE, whereas 5/5 animals in which EEG recording was performed exhibited 10–30 s spontaneous electrographic seizures by 4 weeks after SE (Supplementary Fig. 1). Thus, animals studied at 1–2 d following SE were considered to be in the latent period, whereas animals studied at 28–30 d following SE were considered epileptic. Control groups included animals treated with vehicle (saline) only, PB only, and another group treated with KA that never developed class V seizures. No physiological or immunohistochemical changes were noted in any of the control groups (Supplementary Fig. 2).

I_h is upregulated 1–2 d after status epilepticus

Because excitatory synaptic activity and glutamate receptor activation have been reported to reduce CA1 pyramidal neuron excitability via increases in I_h (Fan et al., 2005; van Welie et al., 2004), we reasoned that status epilepticus might induce a similar increase in I_h. To test the hypothesis that I_h is increased 1–2 d following SE (1–2 d SE), we compared the input resistance, temporal summation of αEPSPs, voltage sag, and resonance frequency between CA1 pyramidal neurons from 1 to 2 d SE and control rats. These physiological measures are sensitive to changes in I_h (Hutcheon et al., 1996; Magee, 1999; Narayanan and Johnston, 2007). Because voltage-dependent conductances active at rest contribute to the intrinsic properties of neurons, all measurements were performed with control and SE neurons held at −70 mV. Input resistance was measured from the voltage response to a family of current injections into either the soma or apical dendrite (Fig. 1A). As expected, the higher density of I_h in the distal dendrites yielded a lower R_N compared to the soma in control CA1 pyramidal neurons. 1–2 d after SE, somatic R_N was significantly reduced by 30% (Fig. 1B). There was also a small but insignificant increase in dendritic R_N. Accordingly, there was no longer a significant difference between the soma and dendrites. If I_h is increased 1–2 d after SE, then there should be more voltage sag during hyperpolarizing injections to the same peak voltage. There was a significant increase in the voltage sag measured at the soma, but not the dendrites, of CA1 pyramidal neurons 1–2 d after SE (Figs. 1C, D). Temporal summation was measured using simulated EPSP-like waveforms (αEPSP, see Materials and methods). A train of 5 αEPSPs at 20 Hz was injected into the soma or dendrite and summation was measured as the percent change in the 5th αEPSP relative to the 1st (Fig. 1E). Changes in I_h can readily be observed as changes in summation at this frequency (Poolos et al., 2002). Although we observed less temporal summation of αEPSPs at 20 Hz than has been previously reported (Poolos et al., 2002), this can be directly attributed to the difference in the parameter α used to generate the αEPSC waveform (0.3 vs. 0.1, see Materials and methods). Nonetheless, temporal summation was less in the distal dendrites of control CA1 pyramidal neurons compared to the soma (Fig. 1F, black bars), consistent with a higher density of I_h. In animals 1–2 d after SE, we observed that temporal summation was decreased in the soma of CA1 neurons as compared to control animals, suggesting an increase in I_h (Fig. 1F). As a result, there was no longer a significant difference between the soma and dendrites, in stark contrast to the observations in control CA1 pyramidal neurons.

Although temporal summation and sag have previously been used as indicators of I_h function, we recently determined that changes in resonance frequency (f_R) is a sensitive indicator of I_h modulation (Brager and Johnston, 2007; Hutcheon and Yarom, 2000; Narayanan and Johnston, 2007). The resonance frequency was identified by the

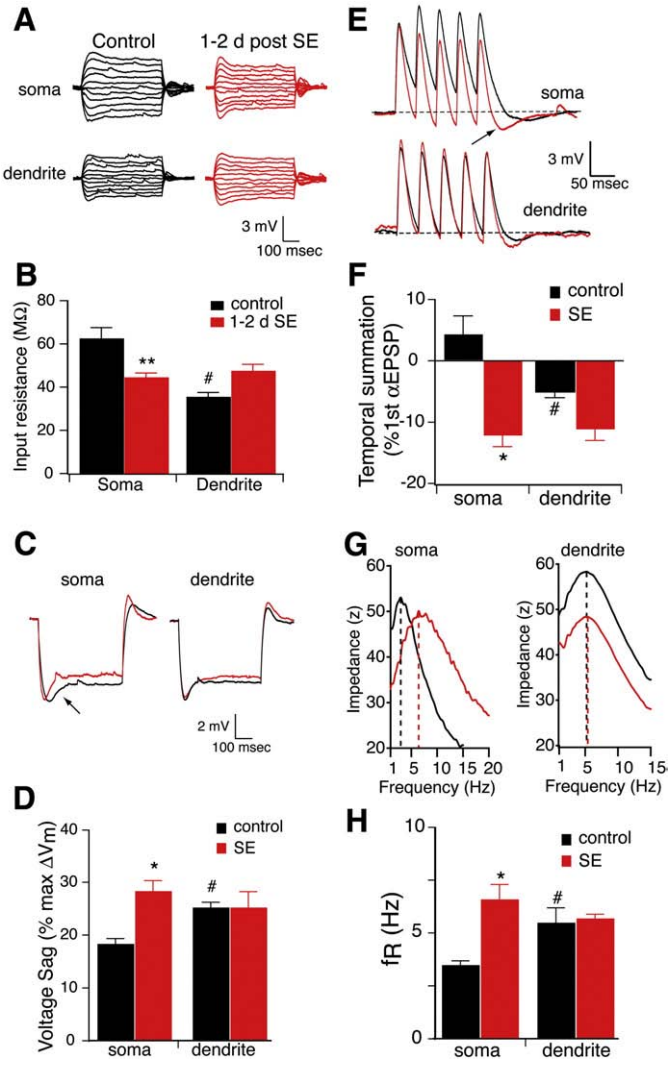

Fig. 1. I_h is increased 1–2 d after a single episode of status epilepticus (SE). (A) Representative traces showing the voltage responses measured at either the soma or dendrite from control (black) or 1–2 d after SE (red) CA1 pyramidal neurons. (B) Summary graph showing that 1–2 d after SE input resistance measured at the soma was significantly reduced compared to control. Note that in control CA1 pyramidal neurons, input resistance was significantly lower in the dendrite compared to the soma. This difference is not present in CA1 pyramidal neurons 1–2 d after SE. $^{**}p<0.01$ compared to control; $^{\#}p<0.05$ compared to soma. (C) Representative traces showing the voltage response to a hyperpolarizing current injection measured at either the soma or dendrite from CA1 pyramidal neurons in control (black) or 1–2 d after SE (red). (D) Summary graph showing that 1–2 d after SE voltage sag measured at the soma was significantly increased compared to control. Note that in control CA1 pyramidal neurons, voltage sag was significantly higher in the dendrite compared to the soma. This difference is not present in CA1 pyramidal neurons 28–30 d after SE. $^{*}p<0.05$ compared to control; $^{\#}p<0.05$ compared to soma. (E) Representative traces showing the voltage response to train of αEPSCs injected and recorded at either the soma or dendrite of control (black) or 1–2 d after SE (red). (F) Summary graph showing that 1–2 d after SE temporal summation measured at the soma was significantly reduced compared to control. Note that in control CA1 pyramidal neurons, temporal summation was significantly lower in the dendrite compared to the soma. This difference is not present in CA1 pyramidal neurons 1–2 d after SE. $^{*}p<0.05$ compared to control; $^{\#}p<0.05$ compared to soma. (G) Representative somatic and dendritic impedance amplitude profile from a control (black) and 1–2 day post SE neuron (red). The dashed lines indicate the resonance frequency (f_R). Note the rightward shift in the SE neuron. (H) Summary graph showing that 1–2 d after SE f_R measured at the soma was significantly increased compared to control. Note that in control CA1 pyramidal neurons, f_R was significantly higher in the dendrite compared to the soma. This difference is not present in CA1 pyramidal neurons 28–30 d after SE. $^{*}p<0.05$ compared to control; $^{\#}p<0.05$ compared to soma.

Please cite this article as: Shin, M., et al., Mislocalization of h channel subunits underlies h channelopathy in temporal lobe epilepsy, Neurobiol. Dis. (2008), doi:10.1016/j.nbd.2008.06.013

maximum of the impedance amplitude profile constructed from the voltage response to injection of the ZAP stimulus (see Materials and methods) into the soma or apical dendrites (Fig. 1G). Consistent with an increase in I_h, somatic f_R was significantly increased 1–2 d after SE compared to control CA1 pyramidal neurons (Fig. 1H). Because increased I_h should lead to membrane depolarization in pyramidal neurons, we also recorded resting membrane potential (V_m) 1–2 d following SE (1–2 d SE). We found that V_m was significantly depolarized 1–2 d after SE compared to control pyramidal neurons (−62±0.8 mV vs. −68±0.3 mV, n=5 for control, n=8 for 1–2 d SE, p<0.001). Taken together, these results indicate that I_h is increased in the somatic region of CA1 pyramidal neurons 1–2 d after SE.

Increased I_h 1–2 d after SE is likely mediated by enhanced HCN1 surface expression

Enhancement of I_h at 1–2 d after SE could reflect an increase in the number of h channels, increased incorporation of preexisting channels into the plasma membrane in the pyramidal neurons, or modification of single-channel properties. Using sensitive and specific α-HCN1 and α-HCN2 antibodies (Shin and Chetkovich, 2007; Shin et al., 2006), we performed western blot analysis on control CA1 tissue extracts as well as extracts prepared from rats 1 d following SE. We found no significant differences in HCN1 protein expression levels in CA1 extract prepared from control CA1 tissue compared to extract prepared 1 d after SE (103.5±5.5%, n=6, p>0.5). A small but significant *reduction* of HCN2 protein expression level was observed (87.0±2.3%, n=6, **p<0.05) (Figs. 2A, B), a finding unexpected in light of increased I_h. No changes in protein expression levels of a housekeeping protein, α-tubulin nor of a neuron-specific isoform of tubulin, β-tubulin III, were detected in CA1 extract of 1 d SE tissues compared to control (α-tubulin; 98.2±2.2%, β-tubulin III; 101.3±5.1%, n=6, p>0.5). We next evaluated h channel surface expression. Ion channel surface expression can be measured by incubating intact neurons with membrane-impermeable reactive biotin, which links covalently to extracellular moieties of membrane proteins (Holman and Henley, 2007). Acute hippocampal slices were prepared from control and 1–2 d SE brains and incubated with sulfo-NHS-LC-biotin for 30 min at 4 °C, followed by lysis and precipitation with immobilized neutravidin. Whereas HCN2 and a control ion channel, GluR1, showed no change in surface expression at 1 d after SE compared to control (control vs. 1 d SE, HCN2; 29.0±1.5% vs. 31.2±2.2%, GluR1; 56.6±3.5% vs. 54.8±2.7%, n=6, p>0.3, Figs. 2C–E), HCN1 showed increased surface expression at 1 d following SE (control vs. 1 d SE, HCN1; 33.5±1.4% vs. 39.3±1.7%, n=6, **p<0.05, Figs. 2C, D). Thus, we conclude that the acute enhancement of I_h we observed in CA1 pyramidal neurons at 1–2 d after SE likely reflects upregulation of surface expression of h channel subunits.

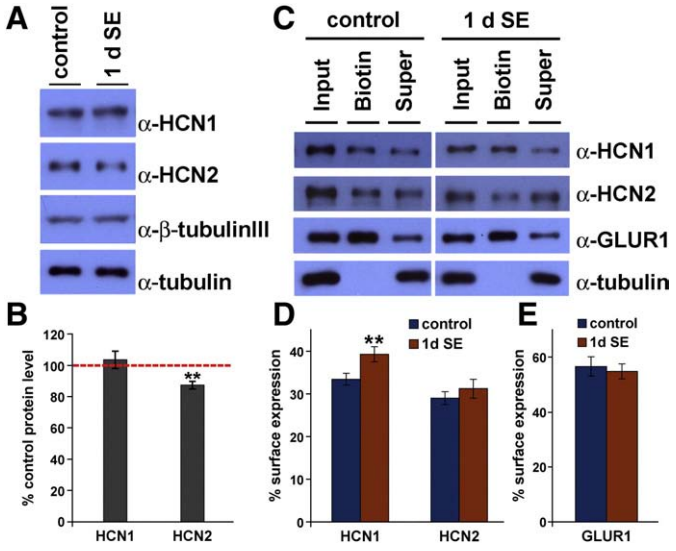

Fig. 2. Surface expression of HCN1 is increased at 1 d after SE. (A) Protein extracts from CA1 of age-matched control and SE animals were separated by SDS-PAGE, and blotted with α-HCN1, α-HCN2. Duplicate blots were labeled with α-tubulin and β-tubulin III (neuron-specific isoform) for loading controls. (B) Intensity of HCN1 and HCN2 bands were quantified and normalized to the intensity of tubulin bands. No significant change in HCN1 protein expression was detected at 1 d after SE (SE, 103.5±5.5%). Slightly decreased HCN2 protein expression was observed at 1 d after SE (87.0±2.3%). (C) Surface expressed proteins in CA1 area hippocampus were biotinylated and precipitated by immobilized neutravidin. Proteins were separated by SDS-PAGE, and blotted with α-HCN1, α-HCN2, α-GluR1 and α-tubulin (as a non-surface control protein). Supernatant represents non-surface fraction of proteins. 30% input was loaded. (D, E) Intensity of HCN1, HCN2 (D) and GluR1 (E) bands were quantified. A significant increase in surface expressed HCN1 proteins, but not HCN2 or GluR1 proteins, was detected at 1 d after SE. See Results section for detailed values. Error bars represent the SEM (n=6, **p<0.05).

Reduced dendritic I_h 28–30 d after SE

We next sought to determine whether h channel function is changed in epileptic hippocampus. We again measured input resistance, temporal summation of αEPSPs, voltage sag, and resonance frequency in CA1 pyramidal neurons from epileptic and control animals. As we observed in the 1–2 d control animals, the higher density of I_h in the distal dendrites yielded a lower R_N compared to the soma. Unlike 1–2 d after SE, 28–30 d after SE, there was no significant change in R_N measured at the soma. However, dendritic R_N increased significantly by 65% (Figs. 3A, B), again resulting in no significant difference between the soma and dendrites. Next, we evaluated the voltage sag as another measurement of I_h. Voltage sag in the dendrites was significantly higher than in the soma of control CA1 pyramidal neurons. In agreement with increased temporal summation, the voltage sag measured in the dendrites of CA1 pyramidal neurons 28–30 d after SE was significantly lower than controls (Figs. 3C, D). Temporal summation of αEPSPs was also significantly less in the dendrites compared to the soma of control CA1 pyramidal neurons (Figs. 3E, F). At 28–30 d after SE, there was no significant difference in temporal summation measured at the soma. However, temporal summation was significantly higher in the dendrites of CA1 pyramidal neurons of 28–30 d SE animals compared to control (Figs. 3E, F). As another measurement of I_h, we evaluated resonance frequency in CA1 pyramidal neurons of control and epileptic brains. In control CA1 pyramidal neurons, the f_R measured in the dendrites was significantly higher than the soma. Consistent with a decrease in I_h at 28–30 d after SE, f_R measured in the dendrites was significantly decreased compared to control CA1 pyramidal neurons (Figs. 3G, H). There was also an increase in f_R measured at the soma although this was not matched by any significant change in input resistance, temporal summation, or voltage sag. Taken together, these results indicate that at 28–30 d following SE, hippocampal pyramidal neurons exhibit a decrease in I_h, primarily manifest in dendrites and either no change or small increase at the soma.

h channels are redistributed from dendrites to soma at 28–30 d after SE

Physiological studies demonstrated a loss of dendritic I_h at 28–30 d after SE, a time point at which KA-treated animals exhibit spontaneous seizures. Reduction of dendritic I_h could result from a reduction in dendritic h channels or modification of h channel conductance or kinetics specifically in dendrites. To evaluate the changes in h channel quantity after SE, we performed western blotting of hippocampal extracts from control or 28 d following SE CA1 tissue. Similar to CA1 extracts prepared 1 d after SE, we found no significant differences in HCN1 or HCN2 levels in CA1 extract prepared from control CA1 tissue or in extract prepared 28 d after SE (98.8±4.4% for HCN1, 88±8.0% for

Please cite this article as: Shin, M., et al., Mislocalization of h channel subunits underlies h channelopathy in temporal lobe epilepsy, Neurobiol. Dis. (2008), doi:10.1016/j.nbd.2008.06.013

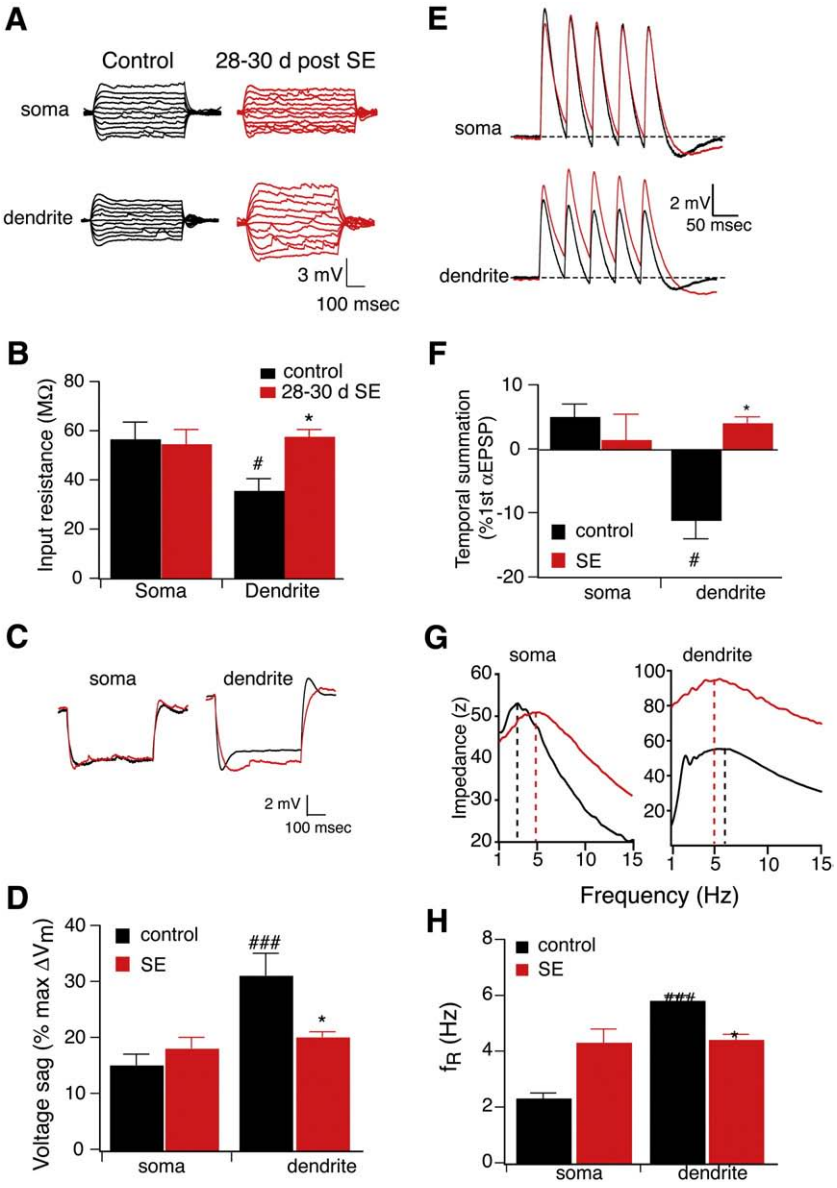

Fig. 3. I_h is decreased 28–30 d after a single episode of status epilepticus (SE). (A) Representative traces showing the voltage responses measured at either the soma or dendrite from control (black) or 28–30 d after SE (red) CA1 pyramidal neurons. (B) Summary graph showing that 28–30 d after SE input resistance measured at the dendrite was significantly reduced compared to control. Note that difference in input resistance between soma and dendrite is not present in CA1 pyramidal neurons 28–30 d after SE. $^{*}p<0.05$ compared to control; $^{\#}p<0.05$ compared to soma. (C) Representative traces showing the voltage response to a hyperpolarizing current injection measured at either the soma or dendrite from CA1 pyramidal neurons in control (black) or 28–30 d after SE (red). (D) Summary graph showing that 28–30 d after SE voltage sag measured at the dendrite was significantly reduced compared to control. Note that difference in voltage sag between soma and dendrites is not present in CA1 pyramidal neurons 28–30 d after SE. $^{*}p<0.05$ compared to control; $^{\#\#\#}p<0.001$ compared to soma. (E) Representative traces showing the voltage response to 20 Hz train of 5 αEPSCs injected and recorded at either the soma or dendrite of control (black) or 28–30 d after SE (red). (F) Summary graph showing that 28–30 d after SE temporal summation measured at the dendrite was significantly increased compared to control. Note that difference in temporal summation between soma and dendrites is not present in CA1 pyramidal neurons 28–30 d after SE. $^{*}p<0.05$ compared to control; $^{\#}p<0.05$ compared to soma. (G) Representative somatic and dendritic impedance amplitude profile from a control (black) and 28–30 day post SE neuron (red). The dashed lines indicate the resonance frequency (f_R). Note the rightward shift in the soma and leftward shift in the dendrite of the SE neuron. (H) Summary graph showing that 28–30 d after SE f_R measured at the soma was significantly increased and f_R measured at the distal dendrite was significantly decreased compared to control. Note that difference in f_R between soma and dendrites is not present in CA1 pyramidal neurons 28–30 d after SE. $^{*}p<0.05$ compared to control; $^{**}p<0.01$ compared to control; $^{\#\#\#}p<0.001$ compared to soma. (For interpretation of the references to colour in this figure legend, the reader is referred to the web version of this article.)

HCN2, $n=6$, $p>0.5$) (Figs. 4A, B). In contrast, levels of another ion channel protein, Kv4.2, were dramatically reduced at 28 d after SE (52.4±3.6%, $n=6$, $^{**}p<0.05$) (Figs. 4A, B), consistent with prior observations of diminished Kv4.2 mRNA and protein levels in area CA1 in epileptic hippocampus (Bernard et al., 2004; Tsaur et al., 1992). There were no differences in protein expression levels of α-tubulin, nor of β-tubulin III, in CA1 extract of 28 d SE tissues compared to control (α-tubulin; 101.6±2.2%, β-tubulin III; 103.7±6.0%, $n=6$, $p>0.5$). These results suggest that whereas the acquired deficiency of Kv4.2 in TLE is a result of diminished Kv4.2 protein expression, the loss of I_h observed at 28–30 d following SE is likely mediated by other mechanisms.

Because I_h changes at 1–2 d after SE are associated with increased HCN1 surface expression, we next evaluated h channel surface expression in epileptic hippocampus by biotinylation assay. Whereas a control ion channel, GluR1, showed no change in surface expression (control vs. 28 d SE, GluR1; 53.3±4.8% vs. 53.4±4.6%, $n=3$, $p>0.5$) (Figs. 4C, E), HCN1 and HCN2 showed profoundly reduced surface expression (control vs. 28 d SE, HCN1; 35.4±2.1% vs. 16.5±1.8%, HCN2; 27.6±1.0% vs. 21.3±1.6%, $n=3$, $^{**}p<0.05$) (Figs. 4C, D). These results

Please cite this article as: Shin, M., et al., Mislocalization of h channel subunits underlies h channelopathy in temporal lobe epilepsy, Neurobiol. Dis. (2008), doi:10.1016/j.nbd.2008.06.013

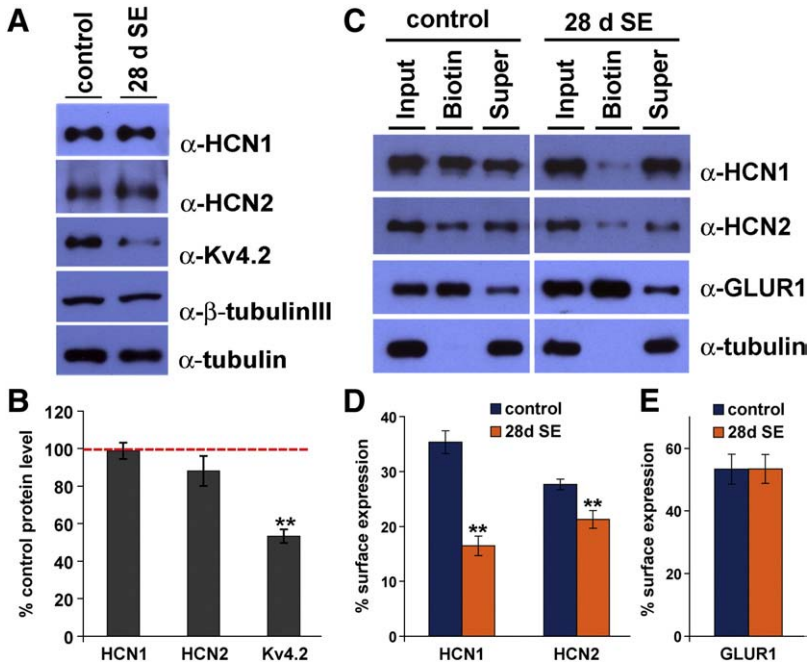

Fig. 4. h channel subunit surface expression is decreased 28 d after status epilepticus. (A) Protein extracts from CA1 of age-matched control and SE animals were separated by SDS-PAGE, and blotted with α-HCN1, α-HCN2, and α-Kv4.2. Duplicate blots were labeled with α-tubulin and β-tubulin III (a neuron-specific isoform) for loading controls. (B) Intensity of HCN1, HCN2 and Kv4.2 bands was quantified and normalized to the intensity of β-tubulin III bands. No significant change in HCN1 or HCN2 protein expression was detected 28 d after SE. Expression of Kv4.2 was decreased by 47.6 ± 3.6% at 28 d after SE. Error bars represent the SEM ($n=6$, $^{**}p<0.05$). (C) Surface expressed proteins in CA1 area hippocampus were biotinylated and precipitated by immobilized neutravidin. Proteins were separated by SDS-PAGE, and blotted with α-HCN1, α-HCN2, α-GluR1 and α-tubulin (as an internalization control). Supernatant represents non-surface fraction of proteins. 30% input was loaded. (D–E) Intensity of HCN1, HCN2 (D) and GluR1 (E) bands were quantified. A significant decrease in surface expressed HCN1 and HCN2 proteins, but not GluR1 proteins was detected at 28 d after SE. See Results section for detailed values. Error bars represent the SEM ($n=3$, $^{**}p<0.05$).

suggest that reduction of I_h observed in CA1 pyramidal neurons at 28–30 d after SE likely reflects reduction of surface expression of h channel subunits.

Because reduction of I_h was largely restricted to the dendrites, we sought to determine if changes in dendritic I_h result from redistribution of channel subunits from distal dendrites. We performed immunolocalization studies to evaluate changes in HCN subunit distribution at 28 d after SE. Interestingly, we found a striking loss of HCN1 immunoreactivity in the distal dendritic fields (SLM) of CA1 pyramidal neurons at 28–30 d following SE (28 d SE). Indeed, the distal enrichment of HCN1 staining was largely abolished, whereas novel HCN1 staining appeared in the soma of CA1 pyramidal neurons ($n=5$ for control and $n=10$ for 28–30 d SE, $^{**}p<0.05$, $^{***}p<0.001$) (Figs. 5A, C). Additionally, while HCN2 subunits remained enriched distally, there was novel HCN2 staining present in the soma ($n=5$ for control and $n=10$ for 28–30 d SE, $^{**}p<0.05$, $^{***}p<0.001$) (Fig. 5B, D). As a control for immunolocalization studies, we evaluated the localization of Kv4.2 and PSD95 in control and epileptic hippocampus. Immunohistochemical staining for Kv4.2 revealed a profound loss of Kv4.2 immunoreactivity throughout CA1, but not in other brain areas (Supplementary Fig. 3), an observation consistent with reduced expression of Kv4.2 (Bernard et al., 2004). On the other hand, evaluation of another prevalent dendritic protein, PSD95, revealed no change in localization at 28–30 d following SE ($n=5$ for control and 28 d SE, $p>0.3$ for all segments) (Figs. 5A, B, E). Because dendritic I_h is reduced in epileptic CA1 pyramidal neurons whereas somatic I_h is unchanged or slightly increased, our biochemical and immunolocalization data suggest that the diminished I_h observed in epileptic hippocampus results from a redistribution of functional distal dendritic h channels to subcellular somatic compartments, leading to a profound reduction in distal dendritic h channels. Furthermore, because HCN2 remains enriched in distal dendrites, these findings suggest that the primary defect is an abnormality associated with HCN1 subunits.

HCN subunit interaction with TRIP8b is disrupted in epileptic hippocampus

Interaction with scaffolding proteins is critical for trafficking numerous ion channels to proper subcellular sites in neurons (Gu et al., 2003, 2006; Leonoudakis et al., 2001; Shibata et al., 2003; Tiffany et al., 2000). Several proteins have been reported to interact with h channel subunits including tamalin, S-SCAM, Mint2, MiRP1, filamin A, vitronectin and the tetratricopeptide repeat (TPR)-containing Rab8b interacting protein (TRIP8b) (Gravante et al., 2004; Kimura et al., 2004; Santoro et al., 2004; Vasilyev and Barish, 2004). Of these, TRIP8b is the only binding partner colocalized with h channel proteins in distal apical dendrites of hippocampal pyramidal neurons, suggesting that TRIP8b may play a unique role in h channel localization (Santoro et al., 2004). To explore whether interaction between h channel subunits and TRIP8b might influence h channel localization in CA1 pyramidal neurons in epileptic hippocampus, we prepared rabbit polyclonal antibodies against the unique N-terminus of TRIP8b, amino acids 1–190 (α-TRIP8b). We confirmed the specificity of α-TRIP8b by western blotting extract prepared from brain and extract of heterologous cells overexpressing GFP tagged TRIP8b. One fraction of α-TRIP8b serum detected a band corresponding to the predicted size of TRIP8b, 78kD, in rat brain (Fig. 6A). Furthermore, immunohistochemical staining with TRIP8b antisera showed that the distinct distal dendritic enrichment in hippocampal and cortical pyramidal neurons shared with HCN1 and in a pattern identical to that published previously (Fig. 6B) (Santoro et al., 2004). We next determined that our antibody effectively immunoprecipitates TRIP8b, and we observed strong coimmunoprecipitation of all three major brain h channel subunits HCN1, 2 and 4 (Fig. 6C). We next explored whether the interaction between TRIP8b and h channel subunits was altered in TLE. In control tissue, TRIP8b coimmunoprecipitated efficiently with both HCN1 and HCN2, and similar strong coimmunoprecipitation of HCN1 and HCN2 was observed in epileptic

Please cite this article as: Shin, M., et al., Mislocalization of h channel subunits underlies h channelopathy in temporal lobe epilepsy, Neurobiol. Dis. (2008), doi:10.1016/j.nbd.2008.06.013

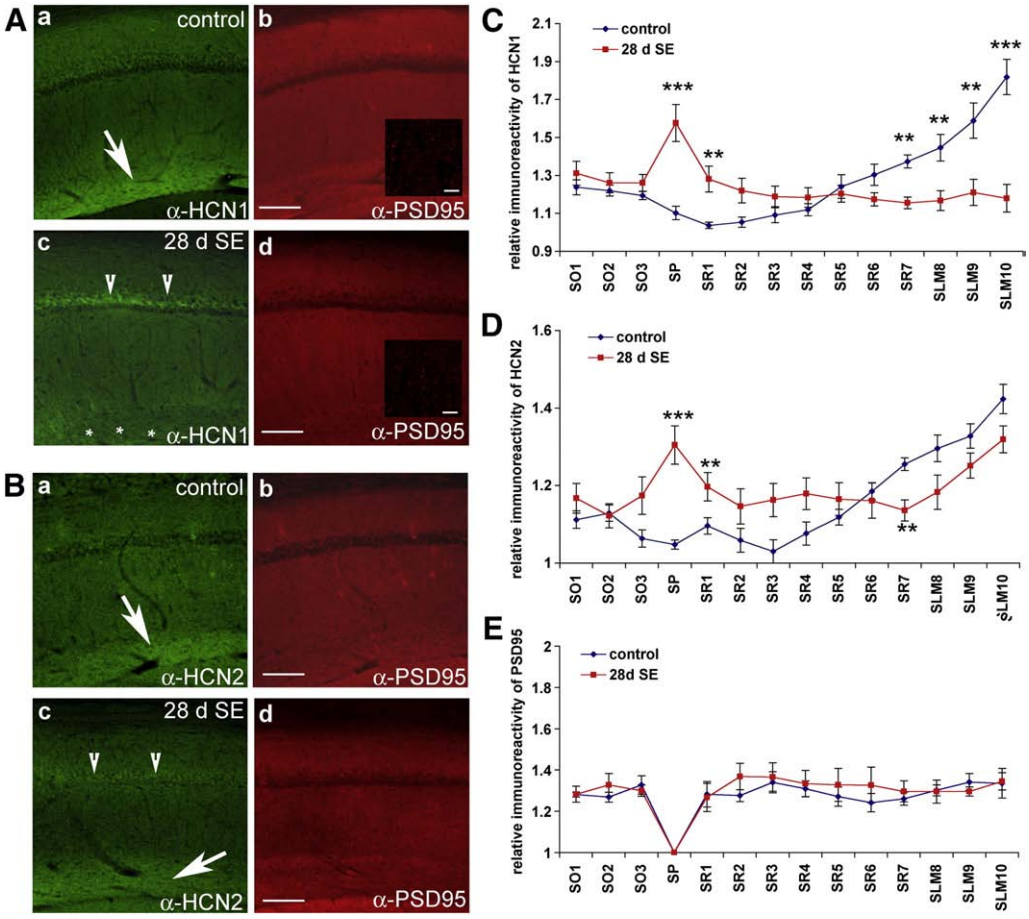

Fig. 5. HCN1 subunits are mislocalized in CA1 28 d after status epilepticus. (A, B) Sagittal sections of control brain [A and B (a, b)] and brain fixed 28 d after SE (28 d SE) [A and B (c, d)] were immunolabeled with gp α-HCN1 or gp α-HCN2 and ms α-PSD95 and visualized with α-gp-alexa488 (left panels, green) and α-ms-cy3 (right panels, red), respectively, for fluorescence staining. HCN1 (A-a, arrow), and HCN2 (B-a, arrow) are both enriched in distal dendritic arborizations within the SLM. The distal dendritic enrichment of HCN1 is lost (A-c, asterisk), whereas high HCN1 immunoreactivity appears in the stratum pyramidale (SP) layer (A-c, arrowheads) of area CA1 of the 28 d SE brains. HCN2 remains enriched in SLM of area CA1 of 28 d SE brain (B-c, arrow), but novel somatic staining is observed (B-c, arrowheads). Note that the distribution pattern of PSD95 is unaltered (A-b, A-d, B-b, B-d), consistent with minimal neuronal damage. Insets (A-b, A-d) are 100× (with 2× digital zoom) images of SLM dendritic fields showing a punctate staining pattern of PSD95, that is similar in 28 d SE and control dendrites of hippocampal area CA1. (C–E) The relative intensity of HCN1 (C), HCN2 (D), and PSD95 (E) immunoreactivity from stratum oriens (SO) to SLM was quantified and graphed. Note the increased HCN1 and HCN2 intensity in soma and decreased HCN1 but not HCN2 intensity in SLM layer 28 d after SE (**$p<0.05$, ***$p<0.001$). Distribution of PSD95 immunoreactivity at 28 d after SE was not significantly different from control. Data points are mean ± SEM of 5 different animals (control) and 10 different animals (28 d SE). Scale bars: 100 μm (5 μm inset). See Materials and methods section for detailed description of the analysis method. (For interpretation of the references to colour in this figure legend, the reader is referred to the web version of this article.)

CA1 extract at 1 d after SE (1 d control vs. 1 d SE; HCN1, 12.6 ± 0.8% vs. 12.0 ± 0.9%; HCN2, 8.8 ± 0.3% vs. 8.8 ± 0.7%, $n=4$, $p>0.7$) (Figs. 7A, B). In contrast, at 28 d following SE, although TRIP8b interaction with HCN2 was preserved, TRIP8b failed to coimmunoprecipitate HCN1 (28 d control vs. 28 d SE; HCN1, 13.4 ± 0.4% vs. 3.2 ± 0.9%; HCN2, 9.9 ± 0.5% vs. 9.1 ± 1.0%, $n=4$, $^{**}p<0.05$) (Figs. 7A, B). If TRIP8b preferentially interacted with HCN2, then reduced TRIP8b protein levels might explain the reduced HCN1 binding in epileptic CA1. However, the protein expression level of TRIP8b was unchanged in epileptic tissues compared to age-matched control (1 d SE, 104.5 ± 9.7%; 28 d SE, 95.6 ± 3.6% from control, $n=4$, $p>0.5$) (Fig. 6D). Thus, loss of the interaction between HCN1 and TRIP8b was not due to altered protein expression level of TRIP8b. Next, we explored TRIP8b localization in epileptic hippocampus. Considering the coimmunoprecipitation data, we anticipated TRIP8b distribution in epileptic hippocampus would resemble HCN2 rather than HCN1. Indeed, TRIP8b immunoreactivity remained enriched in distal dendrites and relatively sparse in the soma of CA1 of epileptic animals (Fig. 6E). In summary, we found that mislocalization of h channel subunits at 28 d after SE in epilepsy occurs independent of changes in TRIP8b localization and that mislocalization of HCN1 is accompanied by dissociation from TRIP8b. These observations suggest that TRIP8b interaction with HCN1 may be critical for h channel trafficking in CA1 pyramidal neuron dendrites, and that yet unknown mechanisms associated with TLE disrupt TRIP8b interaction with HCN1 and lead to h channel mislocalization.

Discussion

The important findings of this study are bidirectional changes in h channel function and localization in CA1 pyramidal neurons in a rat TLE model. The increase of HCN1 surface expression in conjunction with decreased input resistance, decreased EPSP summation, and increased voltage sag suggest that there is an acute increase of I_h within 1–2 d after SE. This is consistent with an anti-excitatory homeostatic response to SE and increased hippocampal network activity. In contrast, reduced h channel subunit surface expression and loss of HCN1 from distal CA1 pyramidal neuron dendrites combined with a reduction in dendritic I_h at 28–30 d following SE suggest a failure of homeostatic h channel regulation in chronic TLE. Furthermore, because h channel mislocalization was associated with disruption of interaction between HCN1 and TRIP8b, these data suggest that

Please cite this article as: Shin, M., et al., Mislocalization of h channel subunits underlies h channelopathy in temporal lobe epilepsy, Neurobiol. Dis. (2008), doi:10.1016/j.nbd.2008.06.013

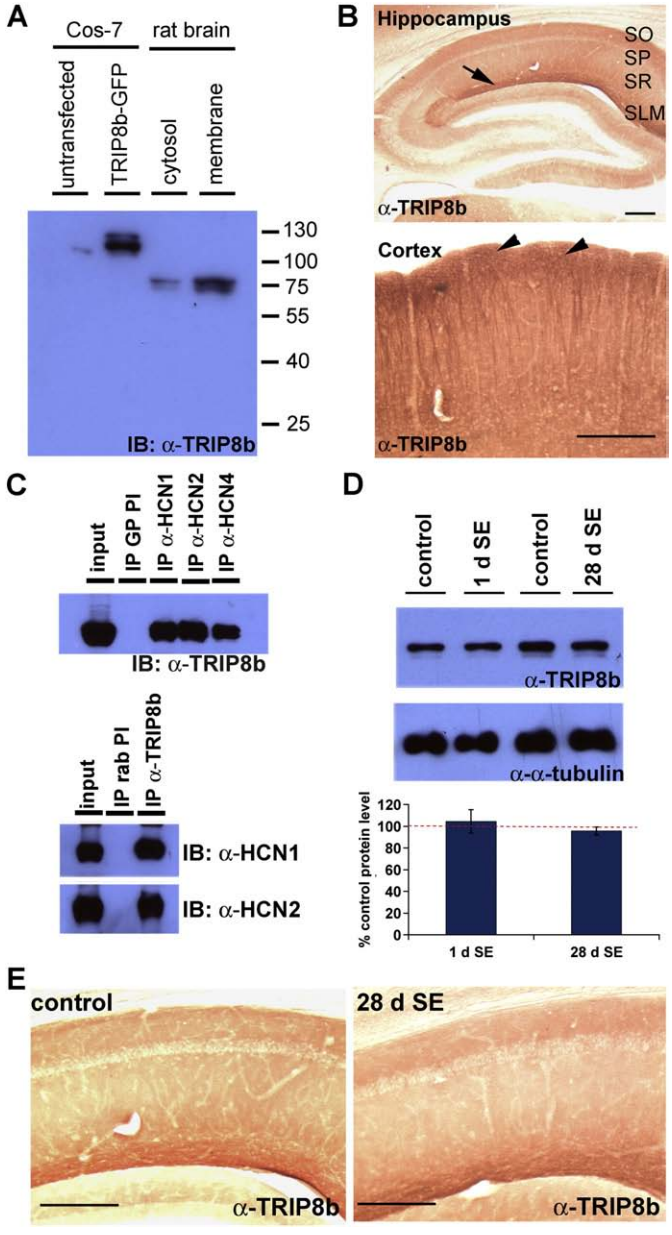

Fig. 6. Expression and distribution of TRIP8b was unchanged in TLE. (A, B) Rabbit α-TRIP8b antibody is specific in biochemical and immunohistochemical assays. (A) Protein extracts from Cos-7 cells transfected with a TRIP8b-GFP-expressing plasmid or rat brain were separated by SDS-PAGE and blotted with α-TRIP8b antibody. Our custom antibody detected a ~110 kDa band in transfected Cos-7 cells and band of ~78 kDa in rat brain, consistent with the predicted size of the GFP-fusion and native protein, respectively. (B) Parasagittal sections of rat brain were immunolabeled with α-TRIP8b antibody. Note the strong immunoreactivity in SLM of hippocampal area CA1 (arrow) and layers I–II of cortex (arrowheads). Scale bars: 200 μm. (SO: stratum oriens; SP: stratum pyramidale; SR: stratum radiatum; SLM: stratum lacunosum moleculare). (C) TRIP8b interacts with h channel subunits in the rat brain. Membrane fractions of rat brain extracts were generated and coimmunoprecipitation performed using antibodies against h channel subunits (top, gp α-HCN1 antibody, gp α-HCN2 antibody, gp α-HCN4 antibody) or α-TRIP8b antibody (bottom). Immunoprecipitation using pre-immune serum (PI) served as a negative control. (D) Protein expression levels of TRIP8b were not altered in the CA1 hippocampus of SE animals. (Top) Hippocampal area CA1 was sub-dissected and membrane extract was generated. Proteins were separated by SDS-PAGE and immunoblotted using α-TRIP8b antibody or ms α-α-tubulin antibody. Protein expression levels of TRIP8b were quantitated by densitometry and normalized with the level of α-tubulin (as a loading control). (Bottom) Graphing the relative density of TRIP8b of SE and non-SE animals shows that TRIP8b protein expression levels were not significantly changed at either 1 d (1 d SE; 104.4 ± 10.8% of 1 d control, $n=4$; $p>0.7$) or 28 d (28 d SE; 95.7 ± 3.7% of 28 d control, $n=4$; $p>0.7$) after SE. (E) Distribution of TRIP8b in CA1 hippocampus was unaltered after SE. 50 μm parasagittal sections of control (left) and 28 d SE (right) brains were immunolabeled with α-TRIP8b antibody and visualized with DAB staining. TRIP8b distribution was not changed in 28 d as compared to control CA1.

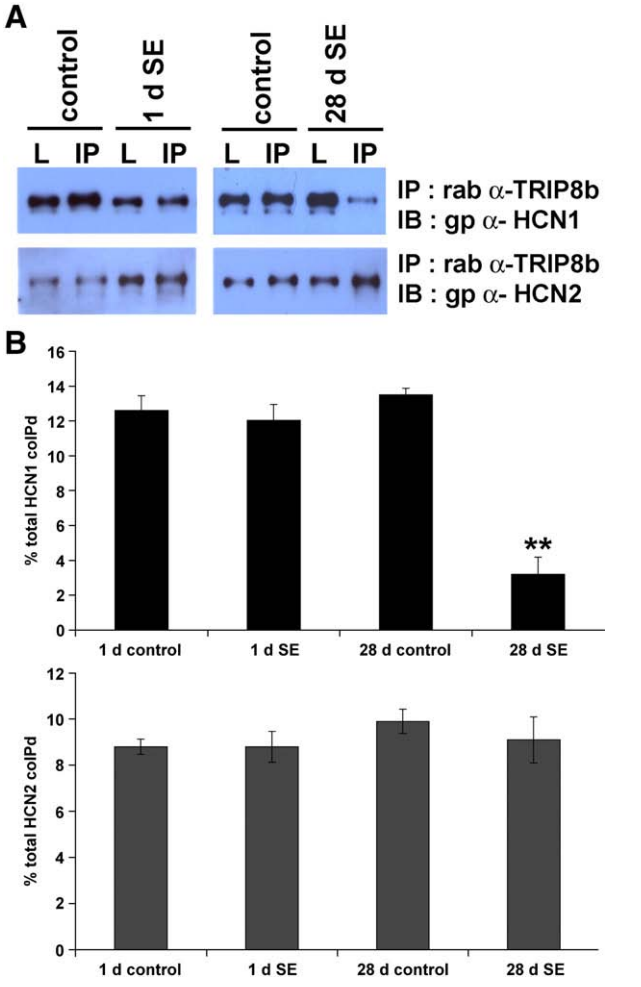

Fig. 7. Interaction between TRIP8b and HCN1, but not HCN2, was disrupted 28 d after SE. (A) Protein extracts of sub-dissected hippocampal area CA1 were generated, then HCN1 and HCN2 were coimmunoprecipitated with TRIP8b using α-TRIP8b antibody. Proteins were separated by SDS-PAGE and immunoblotted with gp α-HCN1 or gp α-HCN2 antibody. (B) Interaction between TRIP8b and h channels was quantitated by densitometry. Interaction between h channels and TRIP8b was not significantly different 1 d after SE (percent coimmunoprecipitated, 1 d control vs. 1 d SE; HCN1: 12.6 ± 0.8% vs. 12.0 ± 0.9%; HCN2: 8.8 ± 0.3% vs. 8.8 ± 0.7%, $n=4$; $p>0.7$). At 28 d after SE, the interaction between TRIP8b and HCN1 was dramatically reduced, whereas interaction with HCN2 was unchanged (28 d control vs. 28 d SE; HCN1: 13.4 ± 0.4% vs. 3.2 ± 0.9 %, $n=4$, $^{**}p<0.05$; HCN2: 9.9 ± 0.5% vs. 9.1 ± 1.0%, $n=4$, $p>0.7$).

abnormal h channel trafficking could contribute to increased hippocampal excitability and seizure propensity in TLE.

Acute upregulation of h channels in TLE

We observed findings similar to Jung et al. in chronic TLE- that I_h is reduced in dendrites in CA1 neurons from epileptic hippocampus (Jung et al., 2007). Although Jung et al. reported decreased protein levels in the pilocarpine model of TLE, we found no changes in h channel subunit protein levels, a difference that may reflect different amounts of cell loss or different effects on transcription in the different TLE models. Indeed, our observation that there were no changes in h channel subunit protein levels at 1–2 d following SE suggests that acute enhancement of I_h in CA1 neurons likely reflects post-translational control of h channels, rather than regulation of h channel subunit transcription or translation. Along these lines, we find a significant upregulation of HCN1 surface expression in CA1 area hippocampus, suggesting that SE provokes increased insertion of HCN1 subunits into the cell membrane or results in decreased internalization. However, other post-translational modifications of h

Please cite this article as: Shin, M., et al., Mislocalization of h channel subunits underlies h channelopathy in temporal lobe epilepsy, Neurobiol. Dis. (2008), doi:10.1016/j.nbd.2008.06.013

channels as a mechanism of altered I_h cannot be excluded. Phosphorylation of ion channel subunits is a mechanism for controlling ion channel function and localization (Levitan, 1994; Mammen et al., 1997; Misonou et al., 2004; Varga et al., 2000). Poolos et al. recently observed that I_h in hippocampal neurons is reduced by blocking p38 mitogen-activated protein kinase (p38 MAPK) (Poolos et al., 2006). Whether p38 MAPK phosphorylates h channel subunits directly to effect changes in I_h and whether P38 MAPK might influence h channel trafficking is unknown, but phosphorylation by p38 MAPK and other protein kinases should be pursued to explore the changes in I_h we observe in TLE.

Chronic downregulation of h channels in TLE

We find compartmentalization of I_h regulation at 28–30 d following SE, with reduced I_h in dendrites but not soma. We also observe a profound loss of surface expressed HCN1 and HCN2 subunits, and mislocalization of h channel subunits. Because total h channel subunits levels remain unchanged and dendritic but not somatic I_h is reduced, these observations suggest relocalization of functional h channels from distal dendrites to a subcellular compartment in the soma. That HCN2 subunits remain enriched in distal dendrites suggests that an abnormality of HCN1 subunit processing is the principle defect in chronic TLE, and that HCN2 subunits colocalized with HCN1 in epileptic pyramidal neuron soma are co-associated in mislocalized heteromeric channels. This interpretation predicts that residual functional h channels in distal dendrites are largely HCN2 homomeric channels. Previously, Brewster et al. reported changes in hippocampal h channel subunit heteromerization in a developmental seizure model (Brewster et al., 2005), and it will be interesting to explore whether heteromerization changes are also important to h channel function in adult rat model of TLE.

h channel trafficking

Many ion channels are targeted to the cell surface and subcellular domains of neurons by interaction with accessory subunits or scaffolding proteins [for review see Lai and Jan, 2006], but protein–protein interactions regulating h channel localization within neurons are yet to be defined. All h channel subunits interact with TRIP8b (Santoro et al., 2004). HCN1 also interacts with the actin binding scaffolding protein, filamin A (Gravante et al., 2004), and HCN2 interacts with the scaffolding proteins tamalin, S-SCAM, and MINT-2 (Kimura et al., 2004). However, the functional consequences of these interactions are unknown. Overexpression of TRIP8b with HCN subunits in heterologous cells or alone in cultured neurons decreases h channel surface expression or I_h, implicating TRIP8b in h channel trafficking (Santoro et al., 2004). TRIP8b is the only h channel interacting protein colocalized with h channels in distal dendrites, and interestingly, TRIP8b remains enriched in distal dendrites of CA1 but not in cortical pyramidal neurons in the HCN1 knockout mouse (Santoro et al., 2004). This observation suggests that TRIP8b may serve as a chaperone that regulates surface membrane trafficking rather than as fixed scaffolding for dendritic h channels, or that association with h channel subunits is necessary for its scaffolding role. We now report that 1) interaction between TRIP8b and HCN1 was markedly reduced at 28 d but not 1 d after SE and 2) TRIP8b remained enriched along with HCN2 in distal dendrites, whereas HCN1 was mislocalized to the soma at 28–30 d after SE. Because HCN2/TRIP8b interactions were preserved after SE, we reason that post-translational modification of HCN1 subunits comprised the principle defect underlying h channel mislocalization in TLE. Further studies are warranted to explore how TRIP8b interaction with different h channel subunits can be differentially regulated in TLE.

Homeostasis vs. epileptogenesis

Numerous conductances in CA1 dendrites are regulated by homeostatic mechanisms, including I_A (A-channels comprised of Kv4.2 subunits) (Varga et al., 2004; Kim et al., 2007), I_K (delayed rectifier Kv currents comprised of Kv2.1 subunits) (Misonou et al., 2006), and I_h (Fan et al., 2005; van Welie et al., 2004). Whereas Kv2.1 subunits maintain homeostatic regulation following SE (Misonou et al., 2006), Kv4.2 transcription and protein expression is diminished in TLE, reflecting a failure of homeostatic mechanisms leading to increased excitability (Bernard et al., 2004). In our present study, enhanced I_h at 1–2 d after SE might contribute to reduced excitability, consistent with a homeostatic response to the massive excitatory network activity of SE or to enhanced hippocampal synaptic activity during the early latent period of hippocampal epileptogenesis. Alternatively, early enhanced I_h could increase excitability, as when upregulated I_h promotes repetitive firing by rebound depolarization in the rat febrile seizures model (Chen et al., 2001). Further studies are required to dissect the effects early I_h changes have on excitability. Similar to a defect in Kv4.2 in epileptic hippocampus, diminished dendritic I_h at 28–30 d after SE suggests failed homeostatic mechanisms. Whereas total cellular I_h levels may influence spatiotemporal integration (Angelo et al., 2007), distal dendritic enrichment of I_h appears particularly critical for controlling excitability and Ca^{++} signaling in distal dendrites (Tsay et al., 2007). Thus, our studies finding overall reduced I_h with prominent distal dendritic loss predicts general and dendritic localization-related contributions to increased excitability in chronic TLE. Whereas the acquired Kv4.2 channelopathy is a failure of transcription, our data demonstrate that post-translational h channel abnormalities, including abnormal protein-protein interactions and channel mislocalization, could contribute to abnormal hippocampal excitability and increased seizure propensity in TLE. Unresolved is the question of whether h channel mislocalization in chronic TLE is a primary defect of epileptogenesis that enhances excitability and increases seizure propensity, or whether the abnormal epileptic hippocampus drives the defect in h channels. We intend to address this issue in future studies. Regardless, understanding this question of causation and the mechanisms governing h channel localization and function is a fundamental biological exploration that may lead to development of novel therapies for medically refractory epilepsy.

Acknowledgments

We thank Alan Lewis, and Won Jun Choi for comments on the manuscript, and Jim Chen, Daniel E. Choi, Felix L. Nunez Santana, Eric Naylor, Ayman Gheith and Jennifer Stern for technical assistance with immunohistochemistry and EEG recording, Dr. Rishikesh Narayanan for assistance with the analysis of cell resonance and Dr. Raymond Chitwood for technical help with the analysis software. This research was supported by grants from the National Institutes of Health (R21 NS052595 to DC) and (MH48432, MH44754, NS37444 to D.J), and from the Partnership for Pediatric Epilepsy Research, which includes the American Epilepsy Society, the Epilepsy Foundation, The Epilepsy Project, Fight Against Childhood Epilepsy and Seizures (f.a.c.e.s.), and Parents Against Childhood Epilepsy (P.A.C.E.).

Appendix A. Supplementary data

Supplementary data associated with this article can be found, in the online version, at doi:10.1016/j.nbd.2008.06.013.

References

Angelo, K., London, M., Christensen, S.R., Hausser, M., 2007. Local and global effects of I (h) distribution in dendrites of mammalian neurons. J. Neurosci. 27, 8643–8653.
Bender, R.A., Kirschstein, T., Kretz, O., Brewster, A.L., Richichi, C., Ruschenschmidt, C., Shigemoto, R., Beck, H., Frotscher, M., Baram, T.Z., 2007. Localization of HCN1

channels to presynaptic compartments: novel plasticity that may contribute to hippocampal maturation. J. Neurosci. 27, 4697–4706.
Bernard, C., Anderson, A., Becker, A., Poolos, N.P., Beck, H., Johnston, D., 2004. Acquired dendritic channelopathy in temporal lobe epilepsy. Science 305, 532–535.
Brager, D.H., Johnston, D., 2007. Plasticity of intrinsic excitability during long-term depression is mediated through mGluR-dependent changes in I(h) in hippocampal CA1 pyramidal neurons. J. Neurosci. 27, 13926–13937.
Brewster, A.L., Bernard, J.A., Gall, C.M., Baram, T.Z., 2005. Formation of heteromeric hyperpolarization-activated cyclic nucleotide-gated (HCN) channels in the hippocampus is regulated by developmental seizures. Neurobiol. Dis. 19, 200–207.
Chen, K., Aradi, I., Thon, N., Eghbal-Ahmadi, M., Baram, T.Z., Soltesz, I., 2001. Persistently modified h-channels after complex febrile seizures convert the seizure-induced enhancement of inhibition to hyperexcitability. Nat. Med. 7, 331–337.
Du, F., Eid, T., Lothman, E.W., Kohler, C., Schwarcz, R., 1995. Preferential neuronal loss in layer III of the medial entorhinal cortex in rat models of temporal lobe epilepsy. J. Neurosci. 15, 6301–6313.
Dudek, F.E., Hellier, J.L., Williams, P.A., Ferraro, D.J., Staley, K., 2002. The course of cellular alterations associated with the development of spontaneous seizures after status epilepticus. Prog. Brain. Res. 135, 53–65.
Engel, J., 1993. Surgical Treatment of the Epilepsies, 2nd ed. Raven Press, New York.
Fan, Y., Fricker, D., Brager, D.H., Chen, X., Lu, H.C., Chitwood, R.A., Johnston, D., 2005. Activity-dependent decrease of excitability in rat hippocampal neurons through increases in I(h). Nat. Neurosci. 8, 1542–1551.
Gravante, B., Barbuti, A., Milanesi, R., Zappi, I., Viscomi, C., DiFrancesco, D., 2004. Interaction of the pacemaker channel HCN1 with filamin A. J. Biol. Chem. 279, 43847–43853.
Gu, C., Jan, Y.N., Jan, L.Y., 2003. A conserved domain in axonal targeting of Kv1 (Shaker) voltage-gated potassium channels. Science 301, 646–649.
Gu, C., Zhou, W., Puthenveedu, M.A., Xu, M., Jan, Y.N., Jan, L.Y., 2006. The microtubule plus-end tracking protein EB1 is required for Kv1 voltage-gated K+ channel axonal targeting. Neuron 52, 803–816.
Holman, D., Henley, J.M., 2007. A novel method for monitoring the cell surface expression of heteromeric protein complexes in dispersed neurons and acute hippocampal slices. J. Neurosci. Methods 160, 302–308.
Hutcheon, B., Miura, R.M., Puil, E., 1996. Models of subthreshold membrane resonance in neocortical neurons. J. Neurophysiol. 76, 698–714.
Hutcheon, B., Yarom, Y., 2000. Resonance, oscillation and the intrinsic frequency preferences of neurons. Trends Neurosci. 23, 216–222.
Jung, S., Jones, T.D., Lugo Jr., J.N., Sheerin, A.H., Miller, J.W., D'Ambrosio, R., Anderson, A.E., Poolos, N.P., 2007. Progressive dendritic HCN channelopathy during epileptogenesis in the rat pilocarpine model of epilepsy. J. Neurosci. 27, 13012–13021.
Kim, J., Clemens, A., Petralia, R., Hoffman, D., 2007. Regulation of Dendritic Excitability by Activity-Dependent Trafficking of the A-Type K+ Channel Subunit Kv4.2 in Hippocampal Neurons. Neuron 54, 933–947.
Kimura, K., Kitano, J., Nakajima, Y., Nakanishi, S., 2004. Hyperpolarization-activated, cyclic nucleotide-gated HCN2 cation channel forms a protein assembly with multiple neuronal scaffold proteins in distinct modes of protein–protein interaction. Genes Cells 9, 631–640.
Lai, H.C., Jan, L.Y., 2006. The distribution and targeting of neuronal voltage-gated ion channels. Nat. Rev. Neurosci. 7, 548–562.
Leonoudakis, D., Mailliard, W., Wingerd, K., Clegg, D., Vandenberg, C., 2001. Inward rectifier potassium channel Kir2.2 is associated with synapse-associated protein SAP97. J. Cell. Sci. 114, 987–998.
Levitan, I.B., 1994. Modulation of ion channels by protein phosphorylation and dephosphorylation. Annu. Rev. Physiol. 56, 193–212.
Lorincz, A., Notomi, T., Tamas, G., Shigemoto, R., Nusser, Z., 2002. Polarized and compartment-dependent distribution of HCN1 in pyramidal cell dendrites. Nat. Neurosci. 5, 1185–1193.
Magee, J.C., 1998. Dendritic hyperpolarization-activated currents modify the integrative properties of hippocampal CA1 pyramidal neurons. J. Neurosci. 18, 7613–7624.
Magee, J.C., 1999. Dendritic Ih normalizes temporal summation in hippocampal CA1 neurons. Nat. Neurosci. 2, 508–514.
Magee, J.C., Johnston, D., 1997. A synaptically controlled, associative signal for Hebbian plasticity in hippocampal neurons. Science 275, 209–213.
Mammen, A.L., Kameyama, K., Roche, K.W., Huganir, R.L., 1997. Phosphorylation of the alpha-amino-3-hydroxy-5-methylisoxazole4-propionic acid receptor GluR1 subunit by calcium/calmodulin-dependent kinase II. J. Biol. Chem. 272, 32528–32533.
Mascott, C.R., Gotman, J., Beaudet, A., 1994. Automated EEG monitoring in defining a chronic epilepsy model. Epilepsia 35, 895–902.
Misonou, H., Menegola, M., Mohapatra, D.P., Guy, L.K., Park, K.S., Trimmer, J.S., 2006. Bidirectional activity-dependent regulation of neuronal ion channel phosphorylation. J. Neurosci. 26, 13505–13514.
Misonou, H., Mohapatra, D.P., Park, E.W., Leung, V., Zhen, D., Misonou, K., Anderson, A.E., Trimmer, J.S., 2004. Regulation of ion channel localization and phosphorylation by neuronal activity. Nat. Neurosci. 7, 711–718.
Narayanan, R., Johnston, D., 2007. Long-term potentiation in rat hippocampal neurons is accompanied by spatially widespread changes in intrinsic oscillatory dynamics and excitability. Neuron 56, 1061–1075.
Notomi, T., Shigemoto, R., 2004. Immunohistochemical localization of Ih channel subunits, HCN1–4, in the rat brain. J. Comp. Neurol. 471, 241–276.
Poolos, N.P., Bullis, J.B., Roth, M.K., 2006. Modulation of h-channels in hippocampal pyramidal neurons by p38 mitogen-activated protein kinase. J. Neurosci. 26, 7995–8003.
Poolos, N.P., Migliore, M., Johnston, D., 2002. Pharmacological upregulation of h-channels reduces the excitability of pyramidal neuron dendrites. Nat. Neurosci. 5, 767–774.
Racine, R.J., 1972. Modification of seizure activity by electrical stimulation. II. Motor seizure. Electroencephalogr. Clin. Neurophysiol. 32, 281–294.
Santoro, B., Chen, S., Luthi, A., Pavlidis, P., Shumyatsky, G.P., Tibbs, G.R., Siegelbaum, S.A., 2000. Molecular and functional heterogeneity of hyperpolarization-activated pacemaker channels in the mouse CNS. J. Neurosci. 20, 5264–5275.
Santoro, B., Wainger, B.J., Siegelbaum, S.A., 2004. Regulation of HCN channel surface expression by a novel C-terminal protein–protein interaction. J. Neurosci. 24, 10750–10762.
Shibata, R., Misonou, H., Campomanes, C.R., Anderson, A.E., Schrader, L.A., Doliveira, L.C., Carroll, K.I., Sweatt, J.D., Rhodes, K.J., Trimmer, J.S., 2003. A fundamental role for KChIPs in determining the molecular properties and trafficking of Kv4.2 potassium channels. J. Biol. Chem. 278, 36445–36454.
Shin, M., Chetkovich, D.M., 2007. Activity-dependent regulation of h channel distribution in hippocampal CA1 pyramidal neurons. J. Biol. Chem. 282, 33168–33180.
Shin, M., Simkin, D., Suyeoka, G.M., Chetkovich, D.M., 2006. Evaluation of HCN2 abnormalities as a cause of juvenile audiogenic seizures in Black Swiss mice. Brain Res. 1083, 14–20.
Tiffany, A.M., Manganas, L.N., Kim, E., Hsueh, Y.P., Sheng, M., Trimmer, J.S., 2000. PSD-95 and SAP97 exhibit distinct mechanisms for regulating K(+) channel surface expression and clustering. J. Cell Biol. 148, 147–158.
Tsaur, M.L., Sheng, M., Lowenstein, D.H., Jan, Y.N., Jan, L.Y., 1992. Differential expression of K+ channel mRNAs in the rat brain and down-regulation in the hippocampus following seizures. Neuron 8, 1055–1067.
Tsay, D., Dudman, J.T., Siegelbaum, S.A., 2007. HCN1 channels constrain synaptically evoked Ca2+ spikes in distal dendrites of CA1 pyramidal neurons. Neuron 56, 1076–1089.
van Welie, I., van Hooft, J.A., Wadman, W.J., 2004. Homeostatic scaling of neuronal excitability by synaptic modulation of somatic hyperpolarization-activated Ih channels. Proc. Natl. Acad. Sci. U. S. A. 101, 5123–5128.
Varga, A.W., Anderson, A.E., Adams, J.P., Vogel, H., Sweatt, J.D., 2000. Input-specific immunolocalization of differentially phosphorylated Kv4.2 in the mouse brain. Learn Mem. 7, 321–332.
Varga, A.W., Yuan, L.L., Anderson, A.E., Schrader, L.A., Wu, G.Y., Gatchel, J.R., Johnston, D., Sweatt, J.D., 2004. Calcium-calmodulin-dependent kinase II modulates Kv4.2 channel expression and upregulates neuronal A-type potassium currents. J. Neurosci. 24, 3643–3654.
Vasilyev, D.V., Barish, M.E., 2004. Regulation of the hyperpolarization-activated cationic current Ih in mouse hippocampal pyramidal neurones by vitronectin, a component of extracellular matrix. J. Physiol. 560, 659–675.
White, H.S., 2002. Animal models of epileptogenesis. Neurology 59, S7–S14.
Wu, K., Leung, L.S., 2003. Increased dendritic excitability in hippocampal ca1 in vivo in the kainic acid model of temporal lobe epilepsy: a study using current source density analysis. Neuroscience 116, 599–616.

Please cite this article as: Shin, M., et al., Mislocalization of h channel subunits underlies h channelopathy in temporal lobe epilepsy, Neurobiol. Dis. (2008), doi:10.1016/j.nbd.2008.06.013